

ANETA SZEWCZYK-NYKIEL, MAREK NYKIEL\*

## ANALYSIS OF THE SINTERING PROCESS OF 316L – HYDROXYAPATITE COMPOSITE BIOMATERIALS

### ANALIZA PROCESU SPIEKANIA BIOMATERIAŁÓW KOMPOZYTOWYCH 316L-HYDROKSYAPATYT

#### Abstract

The 316L-hydroxyapatite biocomposites were produced by the powder metallurgy technology. The properties and microstructure of these materials are affected by the chemical composition of the powders mixture and the sintering temperature. The sintering temperature of 1240°C and hydroxyapatite addition in an amount of 3% of mass obtained the highest density and hardness and smaller open and closed porosity. Hydroxyapatite addition to austenitic stainless steel modified sintering behaviour. During heating the thermal decomposition of hydroxyapatite took place, which led to the formation of a CaO phase. However, phosphorus diffused into the austenitic matrix and was involved in the eutectic transformation.

*Keywords: hydroxyapatite, 316L, biocomposites, microstructure, sintering*

#### Streszczenie

Kompozyty 316L-hydroksyapatyt zostały wytworzone technologią metalurgii proszków. Właściwości i mikrostruktura badanych materiałów uzależnione są od składu chemicznego mieszanki proszków oraz zastosowanej temperatury spiekania. Temperatura spiekania 1240°C i dodatek hydroksyapatytu w ilości 3% wag. pozwalają uzyskać najwyższą gęstość i twardość oraz najmniejszą porowatość otwartą i zamkniętą. Hydroksyapatyt wpływa na przebieg procesu spiekania stali austenitycznej. Podczas nagrzewania następuje rozkład hydroksyapatytu, który prowadzi do powstania fazy CaO. Natomiast fosfor dyfunduje do osnowy austenitycznej, a następnie bierze udział w przemianie eutektycznej.

*Słowa kluczowe: hydroksyapatyt, 316L, biokompozyty, mikrostruktura, spiekanie*

**DOI: 10.4467/2353737XCT.15.178.4383**

\* PhD. Aneta Szewczyk-Nykiel, PhD. Marek Nykiel, Institute of Material Engineering, Faculty of Mechanical Engineering, Cracow University of Technology.

## 1. Introduction

Due to its interesting properties, the hydroxyapatite plays an important role as a biomaterial. It is characterized by the highest biocompatibility and biological activity of all the materials used in medicine. Hydroxyapatite owes these features to the similarity of chemical and phase composition to inorganic phases occurring in human bones and teeth [1–7].

The high degree of osseointegration means that hydroxyapatite can directly connect to the bone. Hydroxyapatite is poorly soluble and slowly reabsorbed in tissues [1]. Years of clinical studies (supported by histological studies) have confirmed the high biotolerance and beneficial effect of hydroxyapatite in the process of healing and rebuilding of bone and its ability to initiate and stimulate the formation processes of living organism bones [2].

The range of hydroxyapatite applications is quite broad and covers dentistry, craniofacial surgery, orthopaedics, otolaryngology and plastic surgery [3].

Due to its origin, mineral hydroxyapatite (in igneous rocks, limestone metamorphic or sedimentary rock phosphate), natural hydroxyapatite (mainly in the bones and teeth of vertebrates) [5–9] or synthetic hydroxyapatite [4] can be distinguished. Synthetic hydroxyapatite is the most commonly used on the large scale. This material is quite expensive and does not show total compatibility between the chemical composition to the bone and teeth of the human body [5]. In addition, we should be aware of the fact that its chemical composition and properties highly depend on the conditions of production. Therefore, attempts have been made to obtain a powder of hydroxyapatite from natural sources. From an economic point of view the use of natural hydroxyapatite is preferable. It can be obtained from natural materials, which are simultaneously waste in animal husbandry such as animal bones (beasts, goats, pigs, sheep), eggshells, as well as from coral skeletons or human teeth [4–8]. Most of the processes for preparing hydroxyapatite are relatively simple, cheap and also ensure repeatability of results. The natural hydroxyapatite (obtained from animal bones) takes over some of the properties of the raw material from which has been produced, such as its chemical composition or structure [7, 9]. It has greater compatibility with the hard tissues of the human body compared to synthetic hydroxyapatite. On the other hand, the use of natural hydroxyapatite causes certain concerns. Mainly because an incorrect extraction process creates the possibility of transferring dangerous diseases such as Creutzfeldt Jakob disease, BSE, HIV, hepatitis B and C and AIDS [5]. Despite this, in recent times many attempts have been made to obtain natural hydroxyapatite.

Despite very good biocompatibility and bioactivity, hydroxyapatite bioceramics have low mechanical properties, particularly a low fracture toughness ( $K_{IC} = 1.1\text{--}1.2 \text{ MNm}^{-1.5}$  compared to the amount of bone  $K_{IC} = 2\text{--}12 \text{ MNm}^{-1.5}$ ), so that its use is essentially limited to perform implants which do not transfer too high a stress [10, 11].

The ease of bonding hydroxyapatite bioceramics to other materials enables new composite materials to be created [1] and it may be a solution to the problem described above. It is no wonder that new materials are continually sought. Trends observed in recent years in the development of biomaterials indicate precisely the increasing importance of composite materials in implantology. The introduction of hydroxyapatite phase directly to the metal phase, associated with the combination of very good biocompatibility and corrosion resistance of hydroxyapatite with a very good strength and susceptibility to deformation of metals is a very good solution. The metal-ceramic composites constitute promising biomaterials for use in medicine for long-term implants (e.g., articular prosthesis, dental implants) [11–13].

Such composite biomaterials can be successfully obtained by powder metallurgy technology as finished products. Plasma sputtering, CVD and other methods to create a layer of hydroxyapatite can be applied on the surface of a metallic biomaterial implant [1, 10, 12].

Several metal-hydroxyapatite composites have been studied. Particular attention has been paid to composites involving titanium [14–16] and austenitic stainless steel [17–21]. Based on an analysis of the results obtained, it can be concluded that the addition of 316L stainless steel to hydroxyapatite has resulted in an improvement in toughness and strength in comparison to pure hydroxyapatite bioceramics. However, the addition of hydroxyapatite to stainless steel has contributed to increasing the biocompatibility, corrosion resistance and also the hardness and wear resistance of stainless steel [17].

Different compositions of the biocomposite stainless steel 316L-hydroxyapatite have been studied thus far [18]. The hydroxyapatite was introduced in amounts of 0 to almost 50% of mass. It can be stated that the composites with higher hydroxyapatite additive (20 and 50% of mass) had higher porosity and thus lower mechanical strength. Due to these properties, the use of these biocomposites has been precluded as a structural element in the human body [18–19]. Also corrosion resistance (in Ringer's solution) of 316L-hydroxyapatite biocomposites decreased with increasing content of hydroxyapatite [19]. From the viewpoint of mechanical properties the amount of hydroxyapatite has to be smaller than 20% of weight.

The powders of 316L stainless steel and hydroxyapatite were used to obtain biocomposites containing 5, 10 and 15%-mass of hydroxyapatite [20]. The reduction of properties for 316L-hydroxyapatite biocomposites prepared by powder metallurgy was also observed. Namely, when the amount of hydroxyapatite in the powder mixture increased up to 15% mass, the sintered density and also hardness of 316L-hydroxyapatite biocomposites decreased, while the open and total porosity increased. The sintered 316L-hydroxyapatite (5% mass) biocomposite obtained the best combination of physical and mechanical properties.

The 316L steel-hydroxyapatite biocomposites were obtained by powder metallurgy technology in the following stages: mixing the powders of AISI 316L steel and natural origin hydroxyapatite, pressing and sintering. The aim of this study was to clarify the effect of the addition of hydroxyapatite on the sintering process of 316L austenitic stainless steel.

## 2. Materials for research

Austenitic stainless steel and hydroxyapatite powders were used as the starting materials. The powder of AISI 316L is the commercially available powder manufactured by Höganäs. This grade is water atomized powder with particle size  $< 150 \mu\text{m}$ . The chemical composition (in mass %) of AISI 316L is following: 17–18 % Cr, 12–13.5% Ni, 2–2.5% Mo, 0.8% Si, 0.1% Mn, 0.03% C and Fe – up to 100%. The natural origin hydroxyapatite powder was obtained by extracting the cortical part of the long bone of the pig. The procedure for preparing the natural hydroxyapatite involves the following steps: cooking bone in distilled water, the mechanical removal of tissues and parts of the spongy bone residue, leaching of organic matter by 4 molar sodium hydroxide solution, rinsing in distilled water until a constant pH, drying at  $120^\circ\text{C}$  to constant weight, and milling [7–8]. The results of a quantitative chemical analysis show that hydroxyapatite powder contained (in % mass): 17.45% P and 39.51% Ca. The value of the Ca/P ratio in the hydroxyapatite was 1.75.

The powders of 316L stainless steel and natural hydroxyapatite were used to prepare the mixtures with the following compositions:

- 316L – 1% mass hydroxyapatite,
- 316L – 3% mass hydroxyapatite,
- 316L – 5% mass hydroxyapatite.

In order to compare the results, pure 316L steel powder was also used for the studies.

### 3. Experimental procedures

The 316L and hydroxyapatite powders (in appropriate mass proportions) were subjected to mixing for 60 minutes in Turbula. The mixtures thus prepared and also powder of 316L were uniaxially pressed in a rigid matrix at a pressure of 600 MPa. Thus cuboidal samples were obtained with dimensions of  $4 \times 4 \times 15$  mm for dilatometric studies. Furthermore cylindrical green compacts of size  $\text{Ø}20 \times 5$  mm were prepared in the same way. They were designed for density, porosity measurements and microstructural studies.

The sintering process took place in a horizontal NETZSCH 402E dilatometer at two temperatures 1180°C and 1240°C. The 402E DIL was used to evaluate the dimensional changes and phenomena occurring during sintering. During the sintering dry (dew point below  $-60^\circ\text{C}$ ) and high purity (99.9992%) hydrogen flowed by measurement system at a rate of 100 ml/min. The sintering time was 60 minutes. The samples were slowly heated to the isothermal sintering temperature at a rate of  $10^\circ\text{C}/\text{min}$ . The same rate was applied during cooling samples from sintering temperature to ambient temperature. The sintering process of the cylindrical compacts was carried out in a Nabertherm furnace under the same conditions.

The density and porosity of cylindrical samples were measured by the water-displacement method (according to the requirements of PN-EN ISO 2738:2001 norm).

The hardness (HRB) was determined. A metallographic study of the sintered specimens was done with Nikon Eclipse ME 600P Light Optical Microscopy and Scanning Electron Microscopy (SEM). Microhardness HV0.01(10s) was measured by means of FM 700 E Microhardness Tester.

Dilatometric investigations were carried out in the horizontal NETZSCH 402E dilatometer.

### 4. Result and discussion

Figure 1 shows the results of sintered density and also relative density measurements of 316L stainless steel and 316L – Hap biocomposites depending on the applied sintering temperature and the amount of hydroxyapatite addition introduced into the powder mixture. The results of open and closed porosity measurements of the same sintered materials are presented in Fig. 2.

The analysis of the above presented results indicates that both sintering temperature and the chemical composition of the powders mixture had an impact on the density and porosity of sintered 316L – Hap biocomposites.

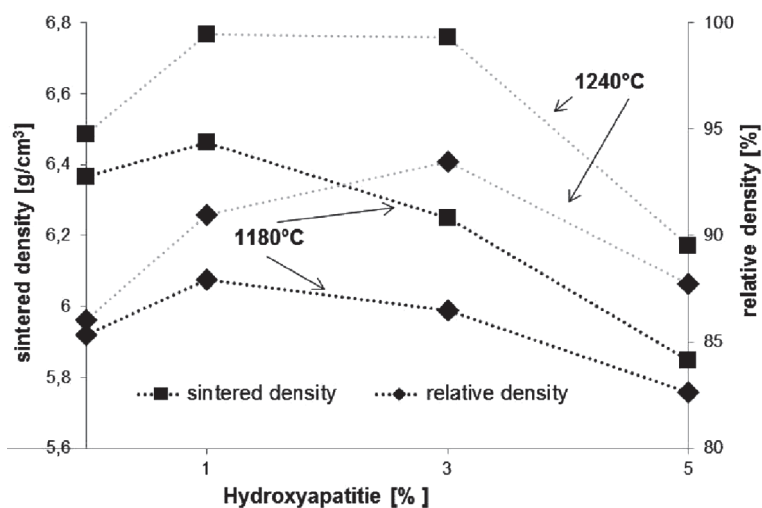


Fig. 1. The influence of sintering temperature and hydroxyapatite addition on density of sintered 316L steel and 316L – Hap biocomposites

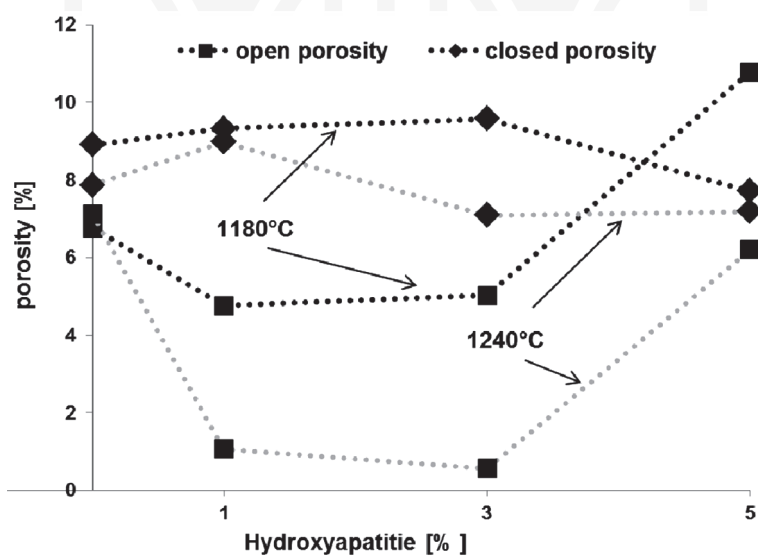


Fig. 2. The influence of sintering temperature and hydroxyapatite addition on porosity of sintered 316L steel and 316L – Hap biocomposites

Regarding the effect of sintering temperature on the physical properties, it can be observed (Fig. 1) that the higher temperature of the sintering process led to much larger values of both sintered density and relative density for all the investigated biocomposites. The same growing trend in density occurred for sintered stainless steel. But the density variation of 316L is not as significant as in the case of the biocomposites studied. Furthermore, it can be

concluded that the increase in the sintering temperature from 1180°C to 1240°C resulted in a decrease in the total, open and closed porosity of sintered 316L – Hap biocomposites and also 316L steel.

As we have already mentioned, the physical properties are significantly affected by the introduction of the hydroxyapatite additive to the material composition. Namely, initially the sintered density and relative density of the biocomposites investigated increases as the amount of hydroxyapatite additive increases up to 1%-mass (in the case of sintering at 1180°C) and 3%-mass (in the case of sintering at 1240°C). Then the densities tend to decline. However, the 316L–5% mass Hap biocomposite shows sintered density below the value obtained for steel 316L.

It should be noted that the effect of the hydroxyapatite addition on the open porosity is just the opposite than in the case of density.

Not only are properties such as density dependent on the sintering temperature and amount of addition of hydroxyapatite. They also decide about hardness as showed results presented in Fig. 3.

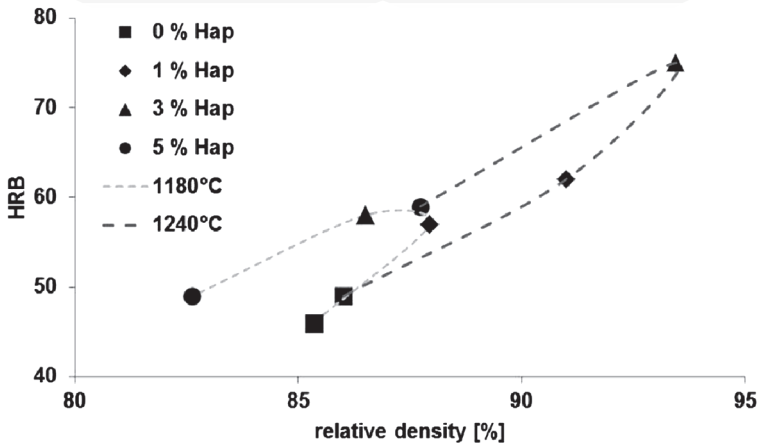


Fig. 3. The influence of sintering temperature and hydroxyapatite addition on relative density and hardness of sintered 316L steel and 316L – Hap biocomposites

For each of the sintering temperatures used the similarity of the relationship between the hydroxyapatite amount and the relative density and hardness of materials obtained can be noted. This means that the initial increase in the content of hydroxyapatite led to an increase in both the density and hardness. The maximum increase in the abovementioned properties occurred in the biocomposite containing hydroxyapatite in amount of 1%-mass sintered at 1180°C. Nevertheless, the combination of the highest values of relative density (93.5%) and hardness (75 HRB) were obtained in the case of 316L-3%-mass hydroxyapatite biocomposite sintered at 1240°C. Further increases in the hydroxyapatite content up to 5% mass meant that the properties were relegated to values comparable to these for sintered 316L steel.

Examples of the microstructures of the materials investigated are presented in Fig. 4-11. The sintered 316L steel (Fig. 4) has an austenitic microstructure. The microhardness of

austenite is about 220 HV 0.01 and 270 HV 0.01 for the steels obtained after sintering at 1180°C and 1240°C respectively.

The introduction of hydroxyapatite addition to 316L steel caused a distinct change in the microstructure of the materials. This is visible in the presented Figures 5–9. The microstructure of the sintered 316L-1%-mass hydroxyapatite material (regardless of sintering temperature) was clearly dual phase. Namely, hydroxyapatite appeared next to the austenite phase. It is also seen in pores disposed at the grain boundaries (Fig. 5, 6). When hydroxyapatite was introduced into the powders mixture in larger quantities (3 and 5%-mass), the microstructure of the sintered biocomposites was dependent on the applied sintering temperature. Namely, there was a heterogeneous eutectic at the grain boundaries of the austenitic matrix (Fig. 7, 9) in the microstructure of sintered at 1240°C biocomposites. Of course, hydroxyapatite was also present. The same microstructure was in 316L-5%-mass hydroxyapatite composites sintered at 1180°C (Fig. 8). Whereas sintered at same temperature 316L-3%-mass hydroxyapatite composite had a dual phase microstructure, as did the sintered 316L-1%-mass Hap biomaterial.

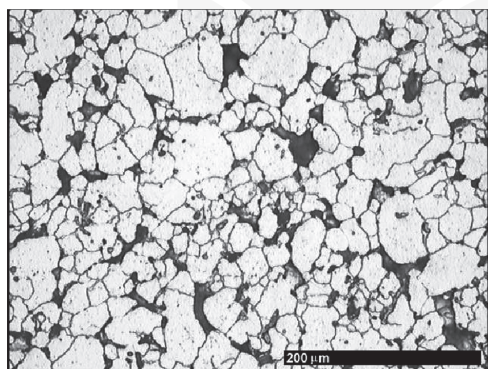


Fig. 4. Microstructure of sintered 316L steel (sintering temperature – 1240°C)

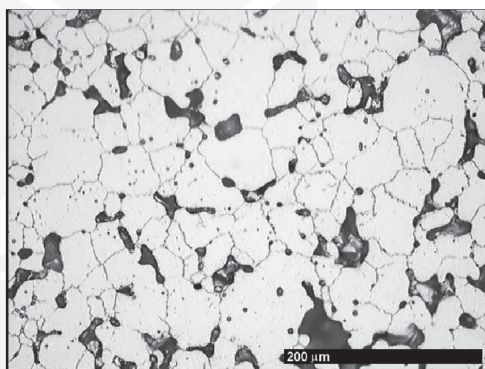


Fig. 5. Microstructure of 316L – 1 mass % Hap (sintering temperature – 1240°C)

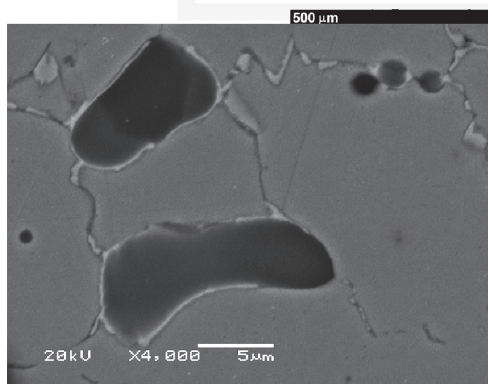


Fig. 6. Microstructure of 316L – 1 mass % Hap (sintering temperature – 1240°C)

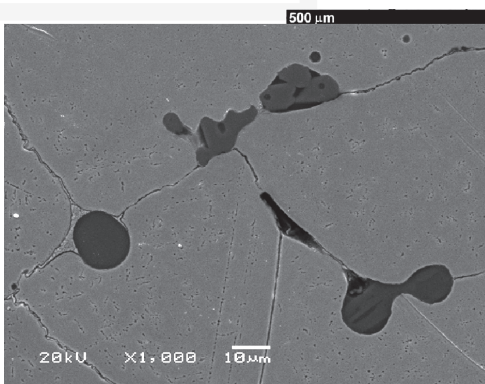


Fig. 7. Microstructure of 316L – 3 mass % Hap (sintering temperature – 1240°C)

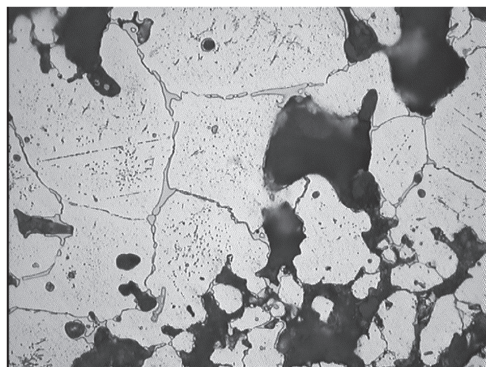


Fig. 8. Microstructure of 316L – 5 mass % Hap (sintering temperature – 1180°C)

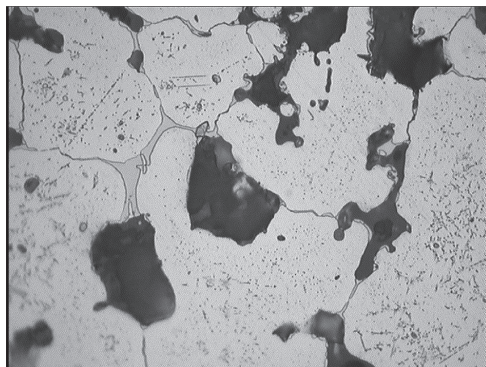


Fig. 9. Microstructure of 316L – 5 mass % Hap (sintering temperature – 1240°C)

The microhardness of austenite in sintered 316L-hydroxyapatite biocomposites was higher than in the sintered 316L stainless steel. And in addition there was an increasing trend of microhardness with the increase of hydroxyapatite addition. For example after sintering at 1240°C, the microhardness of austenite increased from about 220 HV 0.01 up to about 370 HV 0.01. It was expected that the higher hydroxyapatite content in the materials, the higher the share of eutectic, as well as hydroxyapatite phase.

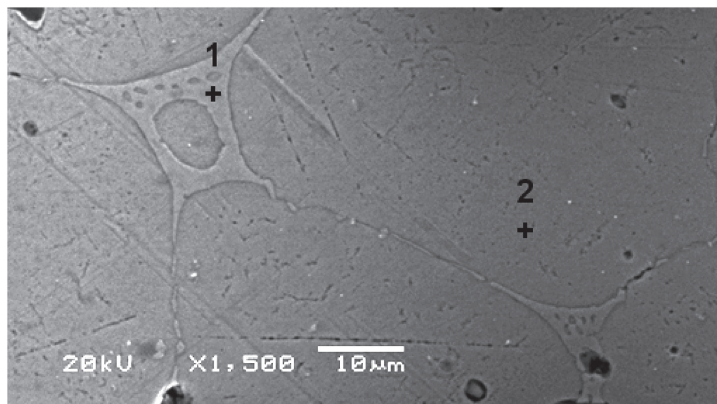
The SEM microstructure of sintered 316L-5%-mass hydroxyapatite biocomposites (obtained after sintering at 1240°C) and the results of the EDAX analysis are presented in Fig. 10. These results of chemical composition microanalysis (performed at point 1 and 2) are shown in the table below the photograph. Point number 2 was designated in the middle of the austenite grain, while point number 1 was on the grain boundary, where the presence of eutectic was previously observed. Microanalysis of the chemical composition indicated that the main elements at point number 2 were Fe, Cr, Ni. Also traces of P appeared. It should be noted that there was no phosphorus in the chemical composition of the 316L steel. This means that the phosphorus diffused from hydroxyapatite into the austenitic matrix (during the sintering process). The main elements in point number 1 are also Fe, Cr, Ni and P. The eutectic occurred on the austenite grain boundaries. It is associated with the Fe – P equilibrium phase diagram.

Figure 11 presents the SEM microstructure of 316L-3%-mass hydroxyapatite biocomposites sintered at 1240°C. The results of the EDAX are shown in the table below photograph. A microanalysis of chemical composition was performed at point number 1. This point was designated in the middle of hydroxyapatite phase that occurred on the grain boundary. There are such elements as O, Ca and also Cr. However, there is no phosphorus. So it is not exactly hydroxyapatite, as presented above. Therefore it is a new phase. The occurrence of the CaO phase is due to the decomposition of hydroxyapatite during the sintering process. It should be emphasized that this is not free CaO. There was a chromium diffusion from the austenitic matrix to the CaO phase.

It is known that the thermal decomposition of hydroxyapatite depends on the chemical formula of the compound, the presence of small additions of other substances, and the partial pressure of water vapour [22–25]. The stoichiometric hydroxyapatite exhibits



thermal stability up to 1350°C [22–24]. Then (according to the equilibrium phase diagram for CaO-P<sub>2</sub>O<sub>5</sub>) the hydroxyapatite decomposes into TTCP (tetracalcium phosphate, Ca<sub>4</sub>P<sub>2</sub>O<sub>9</sub>) and α-TCP (α-tricalcium phosphate, Ca<sub>3</sub>(PO<sub>4</sub>)<sub>2</sub>) at 1350°C. This involves no change in weight.



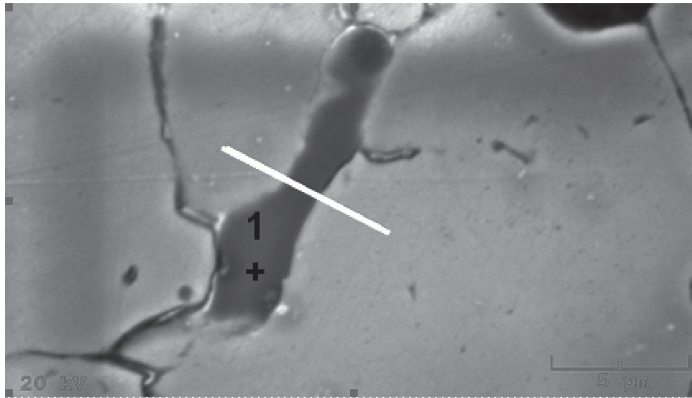
| Elt.    | Line | Intensity (c/s) | Error 2-sig | Conc.  | Units |
|---------|------|-----------------|-------------|--------|-------|
| Point 1 |      |                 |             |        |       |
| P       | Ka   | 251.14          | 5.786       | 23.161 | wt.%  |
| Cr      | Ka   | 295.62          | 6.278       | 32.356 | wt.%  |
| Fe      | Ka   | 243.48          | 5.698       | 37.789 | wt.%  |
| Ni      | Ka   | 22.47           | 1.731       | 6.694  | wt.%  |
| Point 2 |      |                 |             |        |       |
| P       | Ka   | 14.08           | 1.370       | 1.523  | wt.%  |
| Cr      | Ka   | 168.71          | 4.743       | 17.902 | wt.%  |
| Fe      | Ka   | 453.80          | 7.778       | 69.321 | wt.%  |
| Ni      | Ka   | 49.81           | 2.577       | 11.254 | wt.%  |

Fig. 10. The SEM microstructure and microanalysis of chemical composition of sintered 316L – 5 mass % hydroxyapatite (sintering temperature – 1240°C)

However, there is an essential difference between synthetic hydroxyapatite and natural hydroxyapatite (extracted from bovine, pig and human bones). Because the Ca/P ratio is higher than 1.67, natural hydroxyapatite is non-stoichiometric. Moreover, it contains carbonate groups and usually some Mg built into its structure [22, 25]. Some investigators reported that the decomposition of non-stoichiometric hydroxyapatite occurs at temperatures below 1000°C. It was found that the products of this decomposition are different depending on the Ca/P molar ratio of the hydroxyapatite [23].

It was demonstrated [8, 9] that the Ca/P ratio for the hydroxyapatite ceramics sintered at 1200°C was lower than that of material sintered at 800°C. According to the authors

this was due to the occurrence of a CaO phase originating from the decomposition of Hap. It was noticed that the natural hydroxyapatite started to decompose at temperatures above 700°C, while CaO occurrence began at a temperature of approximately 800°C. The content of free CaO quickly increased (up to about 1%) with increasing temperature (to 1000°C). These results are also confirmed in other work. According to Knepper [10], hydroxyapatite is not thermally stable during sintering. Namely, both the hydroxyapatite dehydration and irreversible phase transformations take place in composite materials containing hydroxyapatite.



| Elt.    | Line | Intensity (c/s) | Error 2-sig | Conc.  | Units |
|---------|------|-----------------|-------------|--------|-------|
| Point 1 |      |                 |             |        |       |
| O       | Ka   | 47.84           | 2.525       | 62.563 | wt.%  |
| Ca      | Ka   | 313,21          | 6.462       | 29.392 | wt.%  |
| Cr      | Ka   | 54.30           | 2.691       | 8.045  | wt.%  |

Fig. 11. The SEM microstructure and microanalysis of chemical composition of sintered 316L – 3 mass % hydroxyapatite (sintering temperature – 1180°C)

In the system  $\text{CaO-P}_2\text{O}_5\text{-H}_2\text{O}$  there are many calcium phosphates, which are often the metastable phases. They may occur in the material after a suitable heat treatment. According to the abovementioned phase diagram and the study of the thermal decomposition reaction of hydroxyapatite, some authors have reported that not only calcium phosphate (such as  $\text{Ca}_2\text{P}_2\text{O}_7$ ), but also CaO and  $\text{P}_2\text{O}_5$  may appear during HAP decomposition [24].

Figure 12 presents the concentration distribution of elements (which occurred in the tested material) along the line marked in Fig. 11. This line passed through the austenite grains and modified CaO phase (originating from the decomposition of Hap) located on the boundary. The measurement of concentration of elements does not enable the quantitative chemical composition of the material to be determined, but it is a very convenient method for the observation of even small changes in the concentrations of the elements.

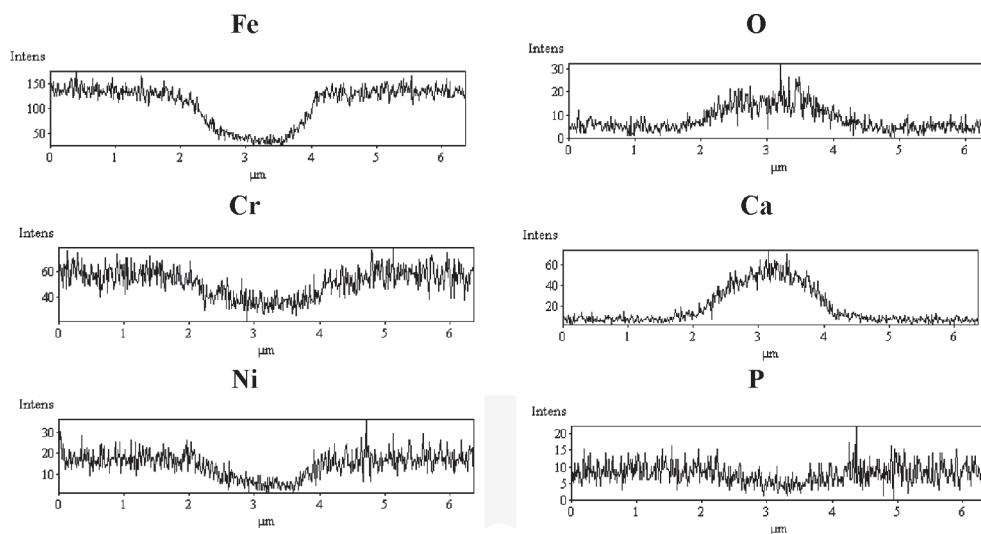


Fig. 12. Concentration distribution of Fe, Ni, Cr, O, Ca and P along a line marked at Fig. 11

It is visible that the concentration distribution of the elements was not the same along the whole length of the measurement line. Namely, the concentration of elements like O and Ca exhibits a marked increase in the area of hydroxyapatite phase occurrence. There is a significant decrease in the concentration of iron, nickel, chromium as well as phosphorus in the phase analysed. This correlates well with the above presented results.

The dilatometric curves of steel 316L and 316L-hydroxyapatite biocomposites recorded during sintering at a temperature of 1240°C are shown in Fig. 13. Analysis of these curves permits the conclusion that hydroxyapatite (depending on the amount introduced into the powder mixture) influences the sintering process of austenitic stainless steel in different ways. Based on the curves presented, the presence of certain points common to all curves and dimensional changes accompanying sintering as a result of occurrence the thermal expansion and sintering shrinkage can be observed.

Initially, as the temperature increases, the thermal expansion of the materials rises, resulting in an increase in sample dimensions. Fig. 13 shows that the presence of hydroxyapatite practically does not contribute to the change in the dimensions of samples in the range of heating from ambient temperature to about 700°C, compared with pure 316L steel. Also the thermal expansion coefficient of 316L-hydroxyapatite biocomposites in this temperature range has a value of about  $1.83 \cdot 10^{-5} [1/^\circ\text{C}]$  regardless of the chemical composition of the powder mixture. The presence of hydroxyapatite modified dimensional changes from a temperature of approximately 800°C, from which composites show less swelling than pure steel. The hydroxyapatite reduces the thermal expansion of the materials. After exceeding a temperature of about 850°C thermal expansion starts to decrease, mechanisms of material transport become active. They cause the occurrence of shrinkage. With time, shrinkage starts to dominate over the expansion of the material and we observe the pronounced peak on the curve. The temperature of this peak is about 1000°C for 316L steel. In the case of 316L-hydroxyapatite is within the range of 905–990°C. The shrinkage of samples starts during heating to the sintering temperature.

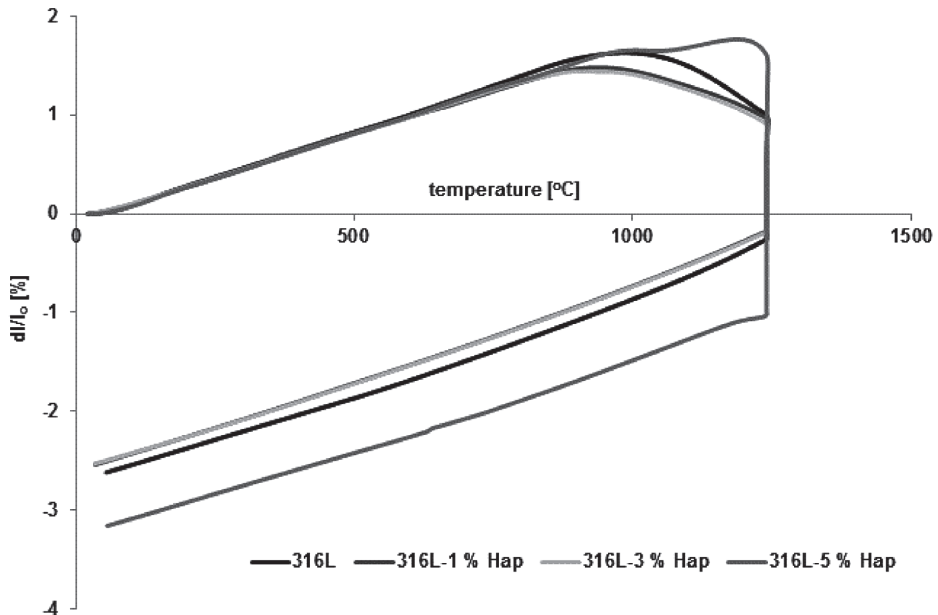


Fig. 13. Dilatometric curves of 316L steel and 316L-hydroxyapatite biocomposites sintered at 1240°C

Because the shrinkage (observed during cooling) is practically the same for all the studied composites (about 2.6 %), the phenomena and processes taking place during isothermal sintering are crucial for the final dimensional changes.

After the whole sintering cycle the highest value of shrinkage was recorded for the sintered 316L-5% mass hydroxyapatite. It equalled 3.16%. This value is significantly larger than the shrinkage observed for other materials. Such a large value of the total shrinkage is associated with a shrinkage occurring during isothermal sintering (Fig. 13), which is caused by the occurrence of a liquid phase. The microstructural studies confirmed the presence of phosphorus in austenite. Hence it can be assumed that there was a reduction of phosphorus oxide with hydrogen during the heating. The analysis of Fe-P equilibrium phase diagram indicates the formation at 1050°C of the eutectic between iron and iron phosphide ( $\text{Fe}_3\text{P}$ ), when the content of phosphorus in the ferrite exceeds 2.8 mass %.

## 5. Conclusion

The 316L-hydroxyapatite biocomposites were obtained using the powder metallurgy technology. The commercially available powder of 316L steel and natural hydroxyapatite (extracted from pig bone) were used. The production process for the samples involved the following steps: mixing powders, pressing and then sintering.

Based on the research results it can be concluded that the properties and microstructure of the sintered biocomposite materials can be changed by selecting of suitable compositions of powder mixture as well as the sintering process parameters.

When the sintering process was carried out at a temperature of 1240°C, the materials under investigation had a higher sintered density, relative density as well as hardness, while the open and closed porosity was lower (compared to the values of these properties obtained after sintering at temperature of 1180°C). Regarding the effect of hydroxyapatite addition on properties, it can be concluded that the combination with the highest values of relative density and hardness and the smaller values of porosity was obtained in the case of 316L-3%-mass hydroxyapatite biocomposite sintered at 1240°C.

Hydroxyapatite addition to austenitic stainless steel modified the sintering behaviour. Namely, the decomposition of hydroxyapatite took place during heating to sintering temperature. This led to the formation of a CaO phase. However, phosphorus diffused into the austenitic matrix and was involved in the eutectic transformation. This was confirmed by the results of the EDAX analysis. It can be observed an austenite matrix, but also heterogeneous eutectic and new phase (formed after the diffusion of chromium to the CaO) on the grain boundaries in the microstructure of 316L-hydroxyapatite biocomposites sintered at 1240°C.

## References

- [1] Sobczak A., Kowalski Z., *Materiały hydroksyapatytowe stosowane w implantologii*, Czasopismo Techniczne, z. 1-Ch/2007, 149–158.
- [2] Dawidowicz A., Pielka S., Paluch D., Kuryszko J., Staniszevska-Kuś J., Solski L., *Zastosowanie mikroanalizy pierwiastkowej do oceny osteindukcyjności i osteokondukcji dokostnych implantów hydroksyapatytowych*, Polimery w medycynie, nr 1, 2005, 1–19.
- [3] Zima A., Paszkiewicz Z., Ślósarczyk A., *Bioceramika TCP ( $\alpha$ TCP,  $\beta$ TCP, BTCP) dla ortopedii i stomatologii – otrzymywanie oraz ocena w testach in vitro*, Materiały Ceramiczne, 62, 1, (2010), 51–55.
- [4] Sobczak-Kupiec A. Wzorek Z., *Właściwości fizykochemiczne ortofosforanów wapnia istotnych dla medycyny – TCP i HAp*, Czasopismo Techniczne, z. 1-Ch/2010, 309–321.
- [5] Elkayer A., Elshazly Y., Assaad M., *Properties of Hydroxyapatite from Bovine Teeth*, Bone and Tissue Regeneration Insights 2009, 2, 31–36.
- [6] Xiaoying L., Yongbin F., Dachun G., Wei C., *Preparation and Characterisation of Natural Hydroxyapatite from Animal Hard Tissues*, Key Engineering Materials, vol. 342–343, 2007, 213–216.
- [7] Haberko K., Bućko M., Mozgawa W., Pyda A., Zarębski J., *Hydroksyapatyt naturalny – preparatyka, właściwości*, Inżynieria Biomateriałów, R. 6, nr 30–33, 2003, 32–37.
- [8] Janus A. M., Faryna M., Haberko K., Rakowska A., Panz T., *Chemical and microstructural characterization of natural hydroxyapatite derived from pig bones*, Microchim Acta, vol. 161, no 3–4, June 2008, 349–353.
- [9] Haberko K., Mirosław M., Bućko., Brzezińska-Miecznik J., Haberko M., Mozgawa W., Panz T., Pyda A., Zarębski J., *Natural hydroxyapatite – its behavior during heat treatment*, Journal of the European Ceramic Society, vol. 26, 2006, 537–542.
- [10] Knepper M., Milthorpe B.K., Moricca S., *Interdiffusion in short-fibre reinforced hydroxyapatite ceramics*, Journals of Materials Science: Materials in Medicine 9, 1998, 589–596.

- [11] Dudek A., Przerada I., *Kompozyty metalowo-ceramiczne do zastosowań w medycynie*, Materiały Ceramiczne, 62, 1, 2010, 20–23.
- [12] Niespodziana K., Jurczyk K., Jurczyk M., *Synteza bio nanomateriałów kompozytowych typu tytan-hydroksyapatyt*, Inżynieria Materiałowa, nr 3/2006, 636–639.
- [13] Szewczyk-Nykiel A., Kazior J., Nykiel M., *Charakterystyka biomateriałów kompozytowych typu AISI 316L-hydroksyapatyt*, Czasopismo Techniczne, z. 2-M/2009, 39–44.
- [14] Balbinotti P., Gemelli E., Buerger A.G., Lima A.S., De Jesus J., Camargo N.H.A., *Microstructure Development on Sintered Ti/HA Biocomposites Produced by Powder Metallurgy*, Materials Research, 14(3), 2011, 384–93.
- [15] Karimi S., Nickchi T., Alfantazi A.M., *Long-term corrosion investigation of AISI 316L, Co-28Cr-6Mo, and Ti-6Al-4V alloys in simulated body solutions*, Applied Surface Science, 258, 2012, 6087–96.
- [16] Silva G., Baldissera M.R., Trichês E.S., Cardoso K.R., *Preparation and characterization of stainless steel 316L/HA biocomposite*, Materials Research, 16(2), 2013, 304–309.
- [17] Miao X., *Observation of microcracks formed in HA-316L composites*, Materials Letters, 57, 2003, 1848–53.
- [18] Silva G., Baldissera M. R., Trichês E., Cardoso K. R., *Preparation and Characterization of Stainless Steel 316L/HA Biocomposite*, Materials Research, 16(2), 2013, 304–309.
- [19] Robin A., Silva G., Rosa J. L., *Corrosion Behavior of HA-316L SS Biocomposites in Aqueous Solutions*, Materials Research, 16(6), 2013, 1254–1259.
- [20] Szewczyk-Nykiel A., Nykiel M., *Study of hydroxyapatite behaviour during sintering of 316L*, Archives of Foundry Engineering, vol. 10, 3/2010, 235–240.
- [21] Szewczyk-Nykiel A., Nykiel M., Kazior J., *Spiekane biomateriały kompozytowe AISI 316l – hydroksyapatyt*, Czasopismo Techniczne, z. 6-M/2012.
- [22] Haberko K., Bućko M., Mozgawa W., Haberko M., Pyda A., *Przemiany hydroksyapatytu pochodzenia naturalnego w podwyższonych temperaturach i wybranych atmosferach*, Inżynieria Biomateriałów, R. 9, nr 58–60, 2006, 35–37.
- [23] Zima A., *Wpływ dodatków modyfikujących na właściwości hydroksyapatytowych wielofunkcyjnych tworzyw implantacyjnych przeznaczonych na nośniki leków*, AGH, Kraków 2007.
- [24] Liao C.J., Lin F.H., Chen K.S., Sun J.S., *Thermal decomposition and reconstitution of hydroxyapatite in air atmosphere*, Biomaterials, 20 (1999), 1807–1813.
- [25] Mezahi F.Z., Oudadesse H., Harabi A., Gal Y., Cathelineau G., *Sintering Effects on Physico Chemical Properties of Bioactivity of Natural and Synthetic Hydroxyapatite*, Journal of the Australian Ceramic Society Volume 47[1], 2011, 23–27.